Calculating Entrainment and Flame Height in Fire Plumes of Axisymmetric and Infinite Line Geometries

BRIAN S. GROVE[1,*] AND JAMES G. QUINTIERE[2]

[1]*Bureau of Alcohol, Tobacco and Firearms, Fire Research Laboratory, Maryland, USA*

[2]*University of Maryland, Department of Fire Protection Engineering, USA*

ABSTRACT: New correlations for flame height and far and near field entrainment are developed from existing data and simple point source theory based on conservation of mass, momentum and energy in the fire plume. These correlations provide prediction of entrainment and flame height for linear sources and for axisymmetric sources. Source geometry and combustion zone radiation heat transfer are incorporated into near field entrainment and flame height correlations. Near field entrainment correlations are compared with other existing correlations and show some differences. Far and near field entrainment correlations for the axisymmetric source are graphed together to show how to calculate entrainment throughout the entire plume. A comparison of entrainment from axisymmetric and infinite line sources of equivalent strength and fuel bed area has also been included.

KEY WORDS: entrainment, flame height, aspect ratio, axisymmetric, infinite line, linear.

INTRODUCTION

THIS PAPER ORIGINATED from a broad study of infinite line plumes in an effort to move the understanding and credibility of line plume correlations to the same engineering comfort level as their axisymmetric counterparts [1]. Line plumes have an aspect ratio, defined as width, D, divided by length, L, that approaches zero. Axisymmetric sources have aspect ratios equal to one. In this study, new theory was developed and fitted to

*Author to whom correspondence should be addressed. E-mail: BSGrove@atfhq.atf.treas.gov

1042-3915/02/03 0117–21 $10.00/0 DOI: 10.1106/104239102029496
© 2002 Society of Fire Protection Engineers

existing data to determine correlations for temperature, velocity, and plume width in both the far field or smoke plume and near field or combustion zone. Correlations for flame height and entrainment were also derived and are the focus of this paper. The theory was developed first for axisymmetric plumes to verify that it was fundamentally correct and later applied to line plumes. For further information regarding the general theory, assumptions, and development of equations, consult the thesis by Grove [1]. The scope of this paper is only to compare and illustrate the use of theoretically-derived empirical correlations for flame height and entrainment. The reader will be shown how to calculate flame height, given a source of certain dimensions and strength. With knowledge of flame height, the reader can then calculate entrainment in both the combustion zone and smoke plume.

NEAR FIELD ENTRAINMENT AND FLAME HEIGHT CORRELATIONS

The approach taken in both regimes is based on the point source model of Morton et al. [2], and the extended analysis by Steward [3] for finite axisymmetric and infinite line fire sources. A constant entrainment coefficient, α, has been assumed similar to the theoretical analyses of Yokoi [4], Zukoski [5], and Lee and Emmons [6].

Derivation of Near Field Entrainment Correlations

In the far field, source geometry is of secondary importance to energy release rate which dominates all processes. However, in the combustion zone, both source geometry and energy release rate play an important role and need to be considered. Derivation of entrainment equations in the near field differs from that of its far field counterpart in two critical ways.

1. The conservation of energy equation differs in the two regimes.
2. The methodology used to develop entrainment equations is not the same.

The conservation of energy equation applied to the far field assumes that all of the energy is released at a single point or line at the fire source, depending on geometry. Whereas the energy equation in the combustion zone assumes that energy is released evenly throughout this zone and that entrained air mixes with the fuel and burns to completion instantaneously.

The methodology used to develop near field entrainment equations differs from its far field counterpart as follows. In the near field or flame zone, the combustion assumptions of Steward [3] are adopted. Finite source effects are ignored to allow for a direct analytical result. More specifically, finite source widths are included but fuel mass or momentum source effects are

ignored. It will be shown that the results produced in this fashion can correlate much of the combustion region effects for finite sources. Its implementation shows, and will be illustrated in this paper, a consistency between flame length and entrainment rates in the combustion zone. Larger entrainment rates are synonymous with short flame lengths and weak entrainment results in tall flames.

Entrainment rates in the flame zone can be predicted with knowledge of flame height. In fact, the empirical entrainment equations in the combustion zone, defined next, were partially derived through flame height data.

The equations shown in Table 1 are presented in a dimensionless format. C_e is a profile constant that changes with the type of integrating profile assumed, i.e., Gaussian, Top Hat, etc. Typically, a radiation loss of 30%, indicative of the fuel type from which empirically fit data was collected, has been incorporated into the constant C_e. C_l is a geometric constant that characterizes plume entrainment. C_l depends only on α and varies significantly for axisymmetric and infinite line sources. α is a dimensionless constant of proportionality that relates centerline plume velocity to entrainment velocity. In the table below, theoretical values determined for the constants are shown first followed by empirical values derived directly from data.

The entrainment equations given in Table 1 depend primarily on source geometry and are unaffected by the power of the source. However, they are affected by the type of fuel through the radiation fraction χ_r found in the Ψ term.

$$\Psi = \frac{(1-\chi_r)\Delta H_c}{c_p T_o s} \tag{1}$$

As an example, during combustion heptane ($\chi_r = 0.33$) loses a larger proportion of its energy to radiation than methyl alcohol ($\chi_r = 0.16$). Assuming both fuels have approximately the same heat of combustion of

Table 1. Near field entrainment correlations: coefficients = theory, experiment.

Axisymmetric ($\chi_r = 0.30$ for Data)	**Infinite Line ($\chi_r = 0.30$ for Data)**
$\dfrac{\dot{m}_e}{\rho_o\sqrt{gDD^2}} = C_e\left(\dfrac{z}{D}\right)^{1/2}\left(1+2C_l\left(\dfrac{z}{D}\right)\right)^2$	$\dfrac{\dot{m}'_e}{\rho_o\sqrt{gDD}} = C_e\left(\dfrac{z}{D}\right)^{1/2}\left(1+2C_l\left(\dfrac{z}{D}\right)\right)$
$C_e = \dfrac{\pi}{2\sqrt{3}}\sqrt{\dfrac{\Psi}{n}}, \quad 0.148 \text{ or } 0.0565\sqrt{\Psi}$	$C_e = \dfrac{\sqrt{\pi}}{2}\sqrt{\dfrac{\Psi}{n}}, \quad 0.148 \text{ or } 0.0565\sqrt{\Psi}$
$C_l = \dfrac{4}{5}\alpha, \quad 0.179$	$C_l = \dfrac{4\alpha}{3\sqrt{\pi}}, \quad 0.444$

air, $\Delta H_a = \Delta H_c/ns$, methyl alcohol will have a larger value of Ψ than heptane. Note, n is defined as the ratio of air entrained into a fire plume to the air used in combustion. A larger value of Ψ inserted into the dimensionless entrainment equations above will result in larger entrainment rates, thus producing smaller flame heights. A qualitative discussion of the physics controlled by Ψ is given below.

Alcohol flames lose a much smaller percentage of their energy to radiation loss than sooty fuels such as heptane. As a result, the temperature of an alcohol flame is greater than that of a heptane flame. Because temperature is inversely proportional to density, alcohol flames are more buoyant than heptane flames and have greater centerline velocities. Because centerline and entrainment velocities are proportional, an alcohol flame can be expected to entrain more air than a heptane flame, all other factors being held equal.

However, in reality, the burning rate of the two fuels is not equal. The qualitative discussion presented above, although accurate, is of secondary importance to burning rate in determining flame height. For large pool fires, i.e., diameters greater than 15 cm, radiation heat transfer controls burning rate. A large heptane pool fire will have a much greater burning rate than a methanol pool fire and therefore will require more air to combust the greater amount of vaporized fuel thus producing larger flame heights.

In Equation (1), s is the stoichiometric air to fuel ratio and n, found in the entrainment constant C_e, is the ratio of air entrained to air involved in combustion. Typical values of n found in the literature range from 5 to 15. From the axisymmetric profile constant, C_e, we found $n = 9.6$ which is in agreement with Taminini [7].

Derivation of Flame Height Correlations

A useful relationship follows that energy release rate be related to the amount of air entrained into the flame zone times the heat of combustion of the amount of that air involved in combustion. For the infinite line:

$$\dot{Q}' = \dot{m}'_e(Z_f) \cdot \frac{\Delta H_c}{ns} \tag{2}$$

Rearranging Equation (2) and substituting for $\dot{m}'_e$, found in Table 1, results in a simple transition from near field entrainment to flame height and the development of the dimensionless energy release rate terms Q^*_D and Q^{**}_D for axisymmetric and infinite line sources, respectively.

$$Q^*_D = \frac{\dot{Q}}{\rho_o T_o c_p \sqrt{g} D^{5/2}} \quad \text{and} \quad Q^{**}_D = \frac{\dot{Q}'}{\rho_o T_o c_p \sqrt{g} D^{3/2}} \tag{3}$$

Table 2. Flame height correlations: coefficients = theory, experiment.

Axisymmetric ($\chi_r = 0.30$ for Data)	**Infinite Line ($\chi_r = 0.30$ for Data)**
$Q_D^* = \left(\frac{Z^*}{D}\right)^{5/2} = C_f \left(\frac{Z_f}{D}\right)^{1/2} \left(1 + 2C_l \left(\frac{Z_f}{D}\right)\right)^2$	$Q_D^{**} = \left(\frac{Z^{**}}{D}\right)^{3/2} = C_f \left(\frac{Z_f}{D}\right)^{1/2} \left(1 + 2C_l \left(\frac{Z_f}{D}\right)\right)$
$C_f = \frac{\pi}{2\sqrt{3}} \frac{(\Psi/n)^{3/2}}{(1-\chi_r)}, \quad 0.152 \text{ or } 0.00590 \frac{\Psi^{3/2}}{(1-\chi_r)}$	$C_f = \frac{\sqrt{\pi}}{2} \frac{(\Psi/n)^{3/2}}{(1-\chi_r)}, \quad 0.152 \text{ or } 0.00590 \frac{\Psi^{3/2}}{(1-\chi_r)}$
$C_l = \frac{4}{5}\alpha, \quad 0.179$	$C_l = \frac{4\alpha}{3\sqrt{\pi}}, \quad 0.444$

Note that combustion efficiency has not been used in the development of our dimensionless energy release rate terms. Actual or chemical values of energy release rate are prescribed allowing for the direct fit of experimental data to our correlations.

The profile constant for entrainment, C_e, has changed to C_f, a profile constant for flame height. (See Table 2.) The geometric constant C_l remains the same for both near field entrainment and flame height. Similar to near field entrainment, the equations in Table 2 are also in a dimensionless format as will all other subsequent equations be unless otherwise specified.

DISCUSSION OF EMPIRICAL CONSTANTS FOR NEAR FIELD ENTRAINMENT AND FLAME HEIGHT

Recall that the equations for flame height and near field entrainment only differ by their profile constants C_e and C_f. Because geometric constants are the same for both near field entrainment and flame height, given the same fuel source, they can be fit to either type of data. Due to a greater amount of flame height data than near field entrainment data and the fact that flame height is easier to measure and generally more accurate than entrainment, we chose to fit the mutual constant C_l to flame height. The flow chart in Figure 1 shows how the empirical constants in Tables 1 and 2 were determined. It should also be noted that the profile constants, C_f and C_e, developed from axisymmetric flame height and entrainment were used in the infinite line correlations respectively because the constants are theoretically similar. The example below compares theoretical and experimental entrainment profile constants for axisymmetric and infinite line sources.

$$\frac{\pi}{2\sqrt{3}} \sqrt{\frac{\Psi}{2}} \cong \frac{\sqrt{\pi}}{2} \sqrt{\frac{\Psi}{n}} \quad \text{or} \quad 0.907 \cong 0.886.$$

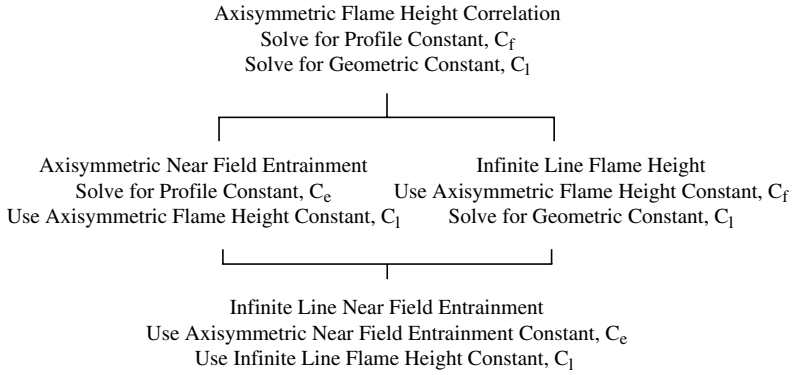

Figure 1. *Derivation chart for near field entrainment and flame height coefficients.*

Figure 1 shows the methodology used to determine empirical coefficients for flame height and entrainment.

Discussion of Axisymmetric Flame Height

The solid line on Figure 2 shows the axisymmetric empirical correlation for dimensionless flame height over diameter Z_f/D versus dimensionless energy release rate, Q^*_D. The constants C_f and C_l were fit to a range of data compiled by Zukoski [5] and represented by the enclosed region on the graph. Burner diameters range from 0.19 to 0.50 m producing fires from 10 to 200 kW. Also placed on the graph, as a dashed curve and a comparison to our equation, is a well-known purely empirical correlation by Heskestad [8]. Heskestad fit his correlation to a subset of the data that we have plotted. Heskestad reports that for low Z_f/D ratios smaller than about 0.5, there is a transition from coherent flaming to distributed flamelets. As a result, data in this area and lower is very scattered. Therefore, correlations in this region are subject to a large degree of freedom allowing for a substantial difference in the rate of decay between the two equations.

It can be shown that the present correlation fits the powers mapped out by Zukoski [9] and shown at the top of the graph. For small Z_f/D corresponding to a weak energy release rate, Zukoski finds that flame height over diameter, Z_f/D, varies with dimensionless energy release rate, Q^*_D, to the 2nd power. Our correlation, found in Table 2, exhibits the same behavior and is explained below. If Z_f/D is small, the first term, "1", in the second set of parentheses becomes dominant. Thus the entire term, in the second set of parentheses, turns into "1" leaving energy release rate to vary with flame height to the ½ power or flame height to vary with energy release rate to the 2nd power as was depicted by Zukoski [9]. On the other extreme, for large Z_f/D ratios

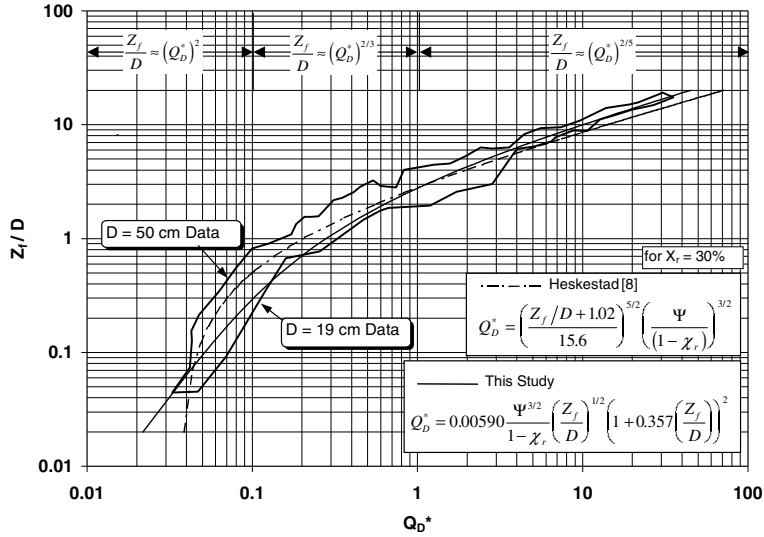

Figure 2. *Axisymmetric smooth fit of dimensionless flame height, Z_f/D, vs. energy release rate, Q_D^*.*

corresponding to a large energy release rate, Zukoski finds that flame height over diameter varies with Q_D^* to the 2/5 power. In our correlation, a large Z_f/D will overwhelm the value of "1" found in the second set of parentheses. Thus, the simplified equation will yield $Z_f/D^{5/2} \approx Q_D^*$ or $Q_D^{*2/5} \approx Z_f/D$ as depicted by Zukoski. Between the two extremes, Zukoski finds $Z_f/D = Q_D^{*2/3}$, but says realistically the exponent could vary anywhere between 2 and 2/5. Zukoski concedes that data between $0.01 \leq Q_D^* \leq 1$ is the least reliable. Most accidental fires occur in this area.

Discussion of Infinite Line Flame Height

Figure 3 shows our flame height correlation for a line source. The correlation is developed by using the same profile constant, C_f, from our axisymmetric flame height correlation and solving for the geometric entrainment constant by choosing a "middle of the road" data point. Data was taken from a variety of sources [3,6,9–13] and includes aspect ratios from 0.1 to 0.007 with 0.01 being the norm. Fuels include methanol, propane, methane, acetone, hydrogen and wood and produce fires ranging from 2.79 to 342 kW/m.

The large gap between the different data sets could be attributed to an individual researcher's definition of flame height or the method with which they took their measurements. As was the case with the data presented by

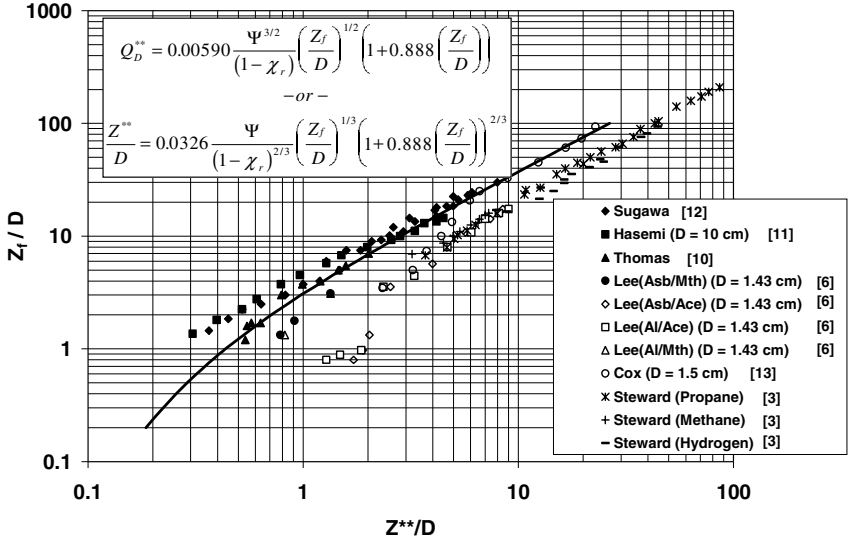

Figure 3. *Dimensionless flame height equation for the infinite line.*

Zukoski in Figure 2 for axisymmetric flame height, sources having large widths or diameters tend to conglomerate at the top left of the data range while those with small diameters or widths are found near the bottom right of the range. This effect is not that important for large Z_f/D ratios where Z^{**} is the dominant term and D has a minimal effect. However, for short flames, found on the lower left section of the graph, the width, D, is the dominant parameter and this effect is extremely important when determining whether or not data is laminar or turbulent. Note, $Q_D^{**} = (Z^{**}/D)^{3/2}$.

One of the problems encountered when developing our empirical correlations was the possibility of fitting constants to laminar flame height data. Our theoretical correlations were developed for purely turbulent data. If laminar data were to contaminate the data pool, it could throw off our empirical constants because several assumptions utilized in developing the theory would no longer be valid. If laminar data is present, it will most likely be found on the right side of the data range where source widths are predominantly small. For this reason our correlation was placed on the upper left cluster of points.

Discussion of Near Field Axisymmetric Entrainment

Figure 4 shows our correlation for entrainment in the flame zone derived from data compiled by Zukoski [5] which includes burners of 0.19 and

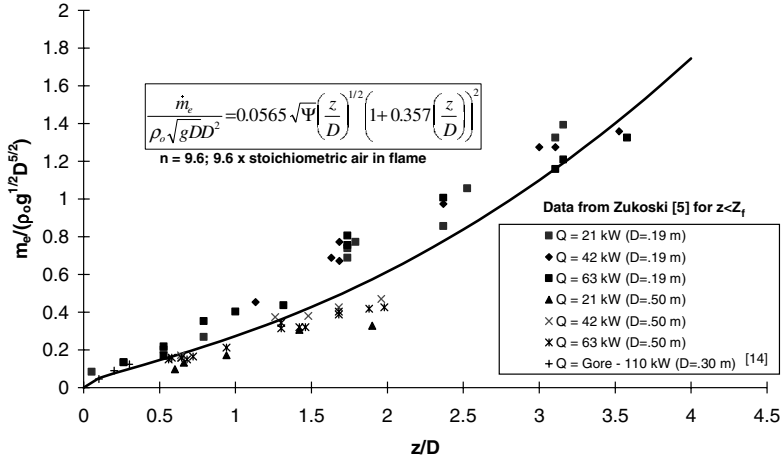

Figure 4. *Near field axisymmetric dimensionless entrainment vs. height (plotted for $X_f = 0.3$).*

0.50 m in diameter and energy release rates of 21, 42, and 63 kW. The correlation was determined by keeping the same geometric constant, C_l, developed from axisymmetric flame height data and solving for C_e. Recently published data by Gore and Zhou [14], using particle-imaging velocimetry, is also included on the graph. Data was only collected at a vertical height very close to the fuel source. Good agreement with Zukoski's data and our correlation is exhibited. For more detailed information on entrainment, Gore and Zhou [14] provide an excellent historical summary of these correlations and their dependence or lack thereof on burner size and energy release rate as well as a review of apparatus that have been used to measure entrainment.

In Figure 5, our correlation is graphed against three others including Thomas [10], Delichatsios [15] and Heskestad [16]. The present correlation differs by 12 and 30% at $z/D = 4$ and 25 and 40% at $z/D = 7$ respectively for Delichatsios' and Thomas' correlations. Most naturally occurring fires have flame heights limited to $Z_f/D = 4$; below this height, agreement is much better than above. Heskestad's linear correlation also exhibits this trend and is in better agreement with the others for low Z_f/D ratios. At Z_f/D ratios greater than 3, Heskestad's correlation substantially over predicts entrainment.

Of the four correlations only Heskestad's is a function of source strength and is often expressed as follows [16]:

$$\dot{m}_{\text{ent}}(\text{kg/s}) = 0.0056\dot{Q}(1 - \chi_r)z/Z_f \tag{4}$$

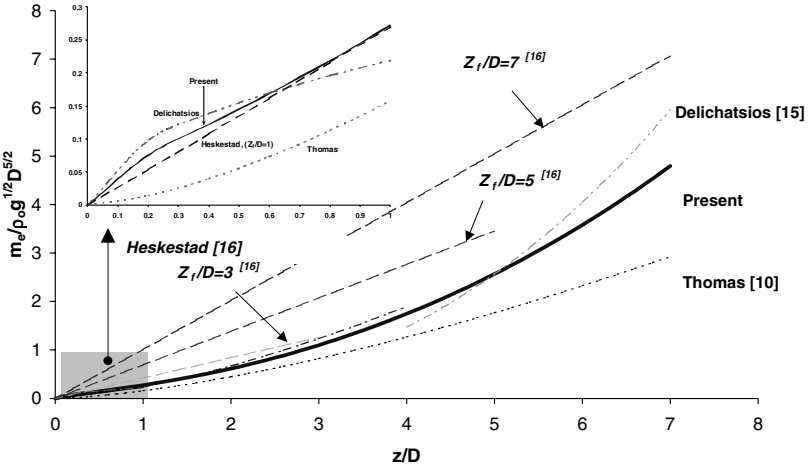

Figure 5. *Comparison of axisymmetric entrainment correlations.*

We have made the equation dimensionless and have assumed the following values:

$$\chi_r = 0.30, \quad c_p = 1.01\,\mathrm{kJ/kg\,K}, \quad T_o = 293\,\mathrm{K}, \quad \rho_o = 1.20\,\mathrm{kg/m^3}$$

The equation is first expressed in terms of dimensionless entrainment and energy release rate. Flame height, Z_f, and height, z, have been normalized with source diameter, D. Finally, dimensionless energy release rate, Q_D^*, is expressed in terms of dimensionless flame height, Z_f/D, using Heskestad's correlation for flame height [16].

$$\frac{\dot{m}_e}{\rho_o\sqrt{g}D^{5/2}} = \frac{1.16Q_D^*(z/D)}{(Z_f/D)} = \frac{1.16((Z_f/D+1.02)/3.89)(z/D)}{(Z_f/D)} \tag{5}$$

Heskestad's correlation can also be found in a dimensionless format including the Fire Froude number [16].

The dependence of Heskestad's entrainment correlation on flame height, and therefore indirectly on energy release rate, requires a separate and distinct correlation be developed for sources of varying Z_f/D ratios. As a result, Heskestad's correlation predicts that tall flames, given the same burner size, will entrain more air than short flames at the same height, z. As an example, for $Z_f/D = 3$ and $Z_f/D = 7$, dimensionless entrainment equals approximately 1 and 3 for $z/D = 3$, respectively. Whereas the other three correlations, which are independent of flame height and energy release rate, predict the same amount of entrainment at a given height no matter what the Z_f/D ratio.

Delichatsios [15] uses the same data as the present authors in addition to data taken by Beyler [17] on 13 and 19 cm burners. Delichatsios breaks the flaming region into three separate regimes rather than developing a correlation that fits the entire combustion zone as the other three correlations.

The three regimes do not meet in one continuous curve. The z/D exponents for Delichatsios match those of the present correlation at the appropriate locations in the fire plume. Delichatsios' near field entrainment correlations are shown below.

$$\begin{aligned}
\frac{\dot{m}_e}{\rho_o\sqrt{g}D^{5/2}} &= 0.219\left(\frac{z}{D}\right)^{1/2} \qquad \frac{z}{D} < 1.0 \\
\frac{\dot{m}_e}{\rho_o\sqrt{g}D^{5/2}} &= 0.237\left(\frac{z}{D}\right)^{3/2} \qquad 1.0 < \frac{z}{D} > 4.0 \\
\frac{\dot{m}_e}{\rho_o\sqrt{g}D^{5/2}} &= 0.0459\left(\frac{z}{D}\right)^{5/2} \qquad \frac{z}{D} > 4.0
\end{aligned} \tag{6}$$

Thomas [10] developed a simple correlation for flame zone entrainment by combining an equation for the conservation of mass, an entrainment coefficient, C, and an equation relating centerline momentum to that of entrained air. The equation was developed as follows:

$$\begin{aligned}
\dot{m}_e &= \rho_o v_e P z \\
\rho_o v_e^2 &= C^2 \rho_f v_f^2 \\
v_e &= C\left(\frac{\rho_f}{\rho_o}\right)^{1/2} v_f \\
v_f &\approx \sqrt{g\frac{\Delta T_f}{T_o}z} \approx \sqrt{gz} \\
\dot{m}_e &= \rho_o C\left(\frac{\rho_f}{\rho_o}\right)^{1/2}\sqrt{gz}Pz \\
&= (\rho_o\rho_f)^{1/2} C\sqrt{g}Pz^{3/2} \\
\dot{m}_e &= C(\rho_o\rho_f g)^{1/2} Pz^{3/2}
\end{aligned} \tag{7}$$

where, v_e is the entrainment velocity; v_f is the flame centerline velocity; P is the perimeter.

The theoretical equation was fit to large fires and yields an empirical coefficient of 0.096 for C.

$$\dot{m}_e = 0.096\,(\rho_o \rho_f\, g)^{1/2} P z^{3/2} \tag{8}$$

Using the simple relation that $\rho_f/\rho_o = T_o/T_f \approx 300\,\mathrm{K}/1000\,\mathrm{K}$ and $\rho_o = 1.21\,\mathrm{kg/m^3}$yields:

$$\dot{m}_e = 0.188 P z^{3/2} \tag{9}$$

The above equation was compared to both axisymmetric and infinite line entrainment equations by substituting the appropriate geometry into the perimeter, P, and making it dimensionless.

For the axisymmetric source:

$$\frac{\dot{m}_e}{\rho_o \sqrt{g} D^{5/2}} = 0.158 \left(\frac{z}{D}\right)^{3/2} \tag{10}$$

For the infinite line source:

$$\frac{\dot{m}'_e}{\rho_o \sqrt{g} D^{3/2}} = 0.100 \left(\frac{z}{D}\right)^{3/2} \tag{11}$$

For both sources, Thomas' [10] correlation entrained the least amount of air out of all the correlations. For large z/D ratios, the gap in entrainment between Thomas' correlation and the others becomes more drastic as Thomas' correlation varies to the 3/2 power and not the 5/2 power as do the present and Delichatsios' [15] correlations. At $z/D = 7$, Thomas' correlation predicts 40% more air entrainment into the fire plume than the present correlation.

Discussion of Near Field Infinite Line Entrainment

Figure 6 shows our line entrainment correlation graphed against its counterpart by Thomas [10]. For this geometry, Thomas' equation also entrains less air than the present correlation. The entrainment and profile constants for the present correlation were taken from infinite line flame height and axisymmetric entrainment data respectively as no reliable data was found with which to fit this correlation. (See Figure 2).

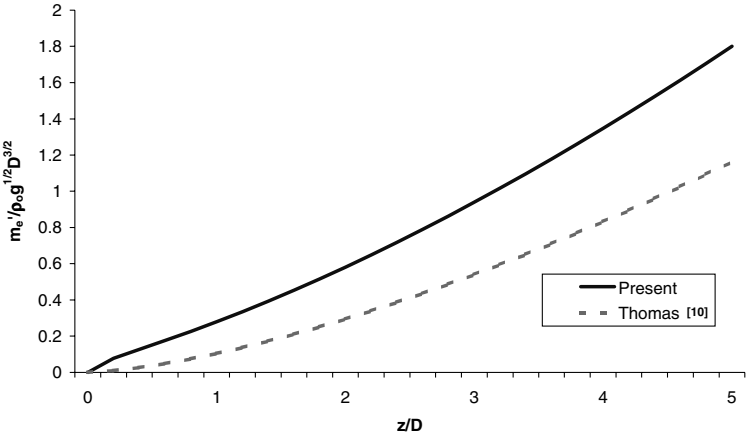

Figure 6. *Near field entrainment for the infinite line.*

FAR FIELD ENTRAINMENT CORRELATIONS

Similar to near field correlations, far field entrainment is given in Table 3a. In this table, ζ is defined as height z (m) divided by a characteristic plume height Z^* (m) and Z^{**} (m) for axisymmetric and infinite line sources, respectively.

$$Z^* = \left(\frac{\dot{Q}}{\rho_o T_o c_p \sqrt{g}}\right)^{2/5} \quad \text{and} \quad Z^{**} = \left(\frac{\dot{Q}'}{\rho_o T_o c_p \sqrt{g}}\right)^{2/3} \tag{12}$$

The constants C_v and C_l found in C_e are from simple point source theory in the far field and correspond to velocity and plume width, respectively. The axisymmetric constants were taken from Yokoi [4] and adjusted to account for a 20% radiation loss that occurs when alcohol is burned. The line constants were derived from unweighted data that was taken from numerous sources and plotted on single variable graphs. A radiation loss of 30% was assigned to the grouping as many of the data points were propane.

Because far field entrainment does not depend on source geometry, as do near field entrainment and flame height, it was made dimensionless by height, z, rather than width, D. However, in order to graph both far and near field entrainment on the same chart, both correlations need to be expressed by the same parameters. Therefore, the above dimensionless far field entrainment correlations are put into the same format as near field entrainment. After multiplying and dividing both sides of the far field entrainment equations by the appropriate power of z and D, respectively, far

Table 3a. Far field entrainment correlations: coefficients = theory, experiment.

Axisymmetric ($\chi_r = 0.20$ for data)	Infinite Line ($\chi_r = 0.30$ for data)
$\frac{\dot{m}_e}{\rho_o\sqrt{g\bar{z}}z^2} = C_e\zeta^{-5/6}$	$\frac{\dot{m}'_e}{\rho_o\sqrt{g\bar{z}}z} = C_e\zeta^{-1/2}$
$C_e = \pi C_v C_l^2, \quad 0.169$	$C_e = \sqrt{\pi}C_v C_l, \quad 0.647$

Table 3b. Far field entrainment correlations, (expressed in near field terms).

Axisymmetric	Infinite Line
$\frac{\dot{m}_e}{\rho_o\sqrt{gD}D^2} = C_e(Q_D^*)^{1/3}\left(\frac{z}{D}\right)^{5/3}$	$\frac{\dot{m}'_e}{\rho_o\sqrt{gD}D} = C_e(Q_D^{**})^{1/3}\left(\frac{z}{D}\right)$
$Q_D^* = \left(\frac{Z^*}{D}\right)^{5/2}$	$Q_D^{**} = \left(\frac{Z^{**}}{D}\right)^{3/2}$

field entrainment is expressed in the same manner as near field entrainment and maintains the same constants. (See Table 3b).

AXISYMMETRIC ENTRAINMENT ILLUSTRATION

Figure 7 illustrates how to calculate entrainment over the entire fire plume for Z_f/D ranging from 0 to 7. As an example, assume $Z_f/D = 4$. The reader would start on the solid line, representing combustion zone entrainment, and take entrainment values up to $z/D = 4$. At this point, the reader has reached the top of the flame zone and must switch to the far field entrainment equation. Entrainment values are then taken in the far field to any desired height.

Far field entrainment correlations were not plotted for $z/D > 7$ on this graph, but the engineer should feel comfortable extending calculations into this regime. Precaution should be taken when doing the same for the near field as this correlation was not fit to data above $Z_f/D = 3.5$. Note that there is only one curve for near field entrainment because it does not depend on flame height. However, there are multiple equations for far field entrainment because the strength of the source has a direct effect on entrainment in the smoke plume.

Note that for $Z_f/D = 3$, our correlation predicts that far field plume entrainment is approximately the same as near field flame entrainment. For $Z_f/D > 3$, smoke plume entrainment is greater than flame entrainment

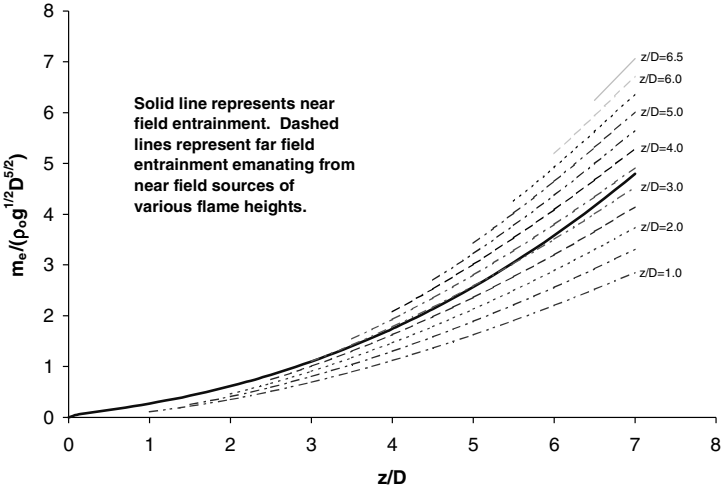

Figure 7. *Near and far field axisymmetric entrainment.*

and, for $Z_f/D < 3$, smoke plume entrainment is less than flame entrainment. The further away from $Z_f/D = 3$ in either direction, the larger the discrepancy between near and far field entrainment. The discontinuity between near and far field entrainment can be attributed to two factors. The intermittent region in a fire plume represents a physical transition that is not defined by either our far or near field entrainment correlations. Additionally, far and near field correlations were developed using different assumptions based on the physics of their entrainment.

INFINITE LINE VERSUS AXISYMMETRIC ENTRAINMENT ILLUSTRATION

The effects of geometry have been incorporated into our entrainment correlations through the conservation equations and dimensionless parameters used to solve them and are obvious on Figure 8. Three source geometries have been plotted including an axisymmetric source, with a 0.357 m diameter, and two infinite line sources of 0.1×1.0 m and 0.01×10 m. The graph was made by first putting the entrainment equations into a dimensional form and solving for flame height to determine at what height near field entrainment equations will yield to far field entrainment equations. Equivalent axisymmetric and line sources were chosen such that both had surface areas of $0.1\,m^2$ and produced 100 kW. This particular burner size, i.e., $0.1\,m^2$, and strength was chosen to maintain consistency with the data used in developing our empirical correlations. A fire source of

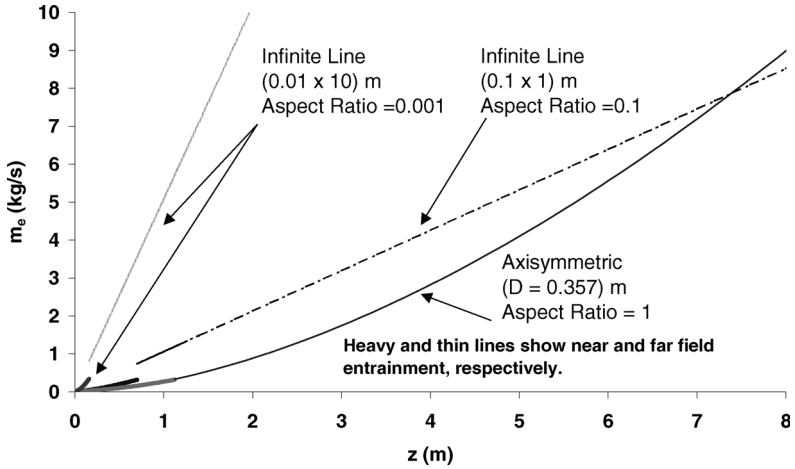

Figure 8. *Comparison of axisymmetric and infinite line entrainment (for same power, 100 kW, and fuel surface area, 0.1 m^2).*

0.01×10 m was not used to develop our correlations nor is expected outside of the laboratory, however this source was included to dramatize entrainment differences between the various geometries.

As expected, the axisymmetric source produces larger flame heights and entrains less air than its linear counterparts as a result of less surface area available for entrainment. Recall that the top of the flaming region occurs where the near field correlation stops and the far field correlation begins. At 2 m and below, the 0.1×1.0 m source entrains more than twice the amount of air as the axisymmetric source. The 0.01×10 m source entrains five times the amount of air as the 0.1×1.0 m source and ten times the amount of air as the axisymmetric source at this height. The discussion below further illustrates the relationship between fire plume surface area and entrainment.

Most fire protection engineers have observed or are aware that if a burner is placed in the corner of a room, it will yield taller flames than if it was placed unobstructed in the center of a room. In a corner, the flame has approximately $\frac{1}{4}$ of the surface area available for entrainment that it would have if it were burning in the open. As a result, fuel vapors have to travel a longer distance to find the oxidizer necessary for their combustion thereby producing taller flames. Although the phenomenon described above is dependent on variables not discussed in this paper, it effectively shows the relationship between fire plume surface area, combustion zone entrainment and flame height.

As height increases, source geometry becomes a less important factor and the gap in entrainment decreases until convergence. The 0.1×1.0 m

and axisymmetric sources both entrain approximately 8 kg/s of air at a height of 7 m. The height at convergence is quite large relative to the size of the sources and, when applied to actual fire scenarios, will most likely be outside the realm of interest. Above this height our equations predict that the axisymmetric source entrains more air; no doubt a manifestation of the equation fit and not what is actually expected.

At a height of 7 m, the 0.01×10 m source entrains three times the amount of air as the above-mentioned sources or 38 kg/s. The disparity in entrainment between the 0.01×10 m source and the other two is still large but has decreased with height. All of the above examples assume substantial buoyancy forces to allow for continued entrainment.

Figure 9 was created using the same methodology as Figure 8. The range of aspect ratios is between 0.2 and 1. The intent of this graph is not to highlight the differences between axisymmetric and infinite line entrainment, as in Figure 8, but to give the reader guidance on when to use either an axisymmetric or infinite line correlation.

Table 4 shows that sources with an aspect ratio of 0.1 entrain substantially more air in both the near and far fields than is predicted using an axisymmetric correlation. It is, therefore, appropriate to use an infinite line correlation on all sources having an aspect ratio of 0.1 and less. However, for aspect ratios greater than 0.1, that are not axisymmetric, the most accurate prediction of entrainment would be to use a rectangular correlation, which has not been presented here. See Quintiere [1] for a discussion of flame height and far and near field entrainment for rectangular sources. If the reader chooses not to use a rectangular correlation, Table 4

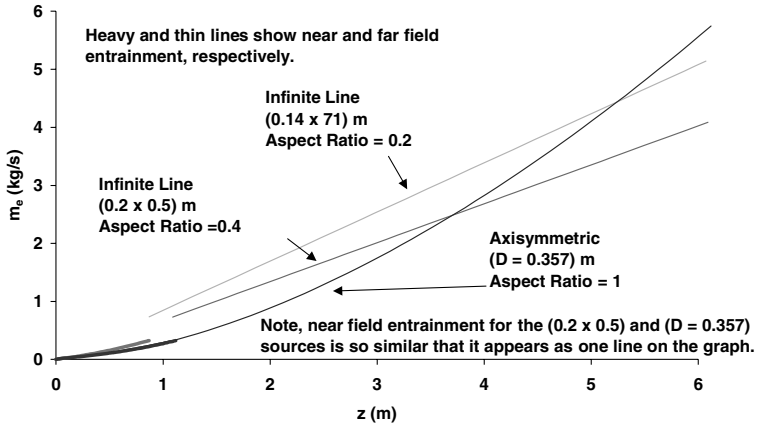

Figure 9. *Comparison of axisymmetric and infinite line entrainment (for same power, 100 kW, and fuel surface area, 0.1 m^2).*

Table 4. Comparison of entrainment values.

Aspect Ratio (D/l)	Source Dimensions (m)	Near Field Entrainment (kg/s)		Far Field Entrainment (kg/s)			
		@ $z = 0.12$ m	% Difference @ $z = 0.12$ m	@ $z = 2$ m	% Difference @ $z = 2$ m	@ $z = 4$ m	% Difference @ $z = 4$ m
1	$D = 0.357$	0.0298	0	0.888	0	2.83	0
0.4	0.2×0.5	0.0285	−4.36	1.34	50.9	2.68	−5.30
0.2	0.14×0.71	0.0327	9.73	1.69	90.3	3.39	19.8
0.1	0.1×1	0.0385	29.1	2.13	140	4.26	50.5

Table 5. Comparison of flame height values.

Aspect Ratio (D/l)	Source Dimensions (m)	Flame Height (m)	
			% Difference
1	$D = 0.357$	1.12	0
0.4	0.2×0.5	1.09	−2.68
0.2	0.14×0.71	0.871	−22.2
0.1	0.1×1	0.706	−36.9

suggests that an appropriate simplification would be to apply an axisymmetric correlation to fires with an aspect ratio of 0.4 and greater and an infinite line correlation to fires with an aspect ratio less than 0.4.

A comparison of flame heights has also been made for sources having aspect ratios between 1 and 0.1. Table 5 also suggests that axisymmetric correlations be applied to sources with aspect ratios of 0.4 and greater and that infinite line correlations be applied to sources with aspect ratios less than 0.4. Note that applying an axisymmetric correlation to all sources will over estimate flame height and is, therefore, conservative.

CONCLUSION

New correlations for entrainment and flame height have shown that applying equations for axisymmetric fires to fires with linear geometries will over predict flame height and under predict entrainment. Future work should include the acquisition of infinite line entrainment data to validate our linear entrainment correlations. New experimental coefficients could then be compared to the coefficients captured from axisymmetric sources to verify the relationships that the authors have established based on theory.

NOMENCLATURE

c_p = specific heat (kJ/kg K)
C = generic constant used in power series
D = axisymmetric diameter or line width (m)
g = gravity (9.81 m/s^2)
L = line length (m)
$\dot{m}$ = mass flow rate (kg/s)
n = ratio of air entrained into fire plume to air involved in combustion
P = perimeter (m)
$\dot{Q}$ = energy release rate (kW)
s = stoichiometric air to fuel ratio
T = temperature (K)
v = velocity (m/s)
z = vertical direction, height (m)
Z_f = flame height (m)
Z^* = characteristic axisymmetric height (m)
Z^{**} = characteristic infinite line height (m)
Q_D^* = characteristic axisymmetric height, $(Z^*/D)^{5/2}$
Q_D^{**} = characteristic infinite line height, $(Z^{**}/D)^{3/2}$

Greek Symbols

α = dimensionless entrainment coefficient, relates center-line plume velocity to entrainment velocity
β = Gaussian profile constant
χ_r = radiation loss fraction
ΔH_c = heat of combustion (kJ/kg)
ΔH_a = heat of combustion of air (kJ/kg)
ΔT = change in temperature (K)
Ψ = fuel burning constant
ρ = density (kg/m^3)

Subscripts

e = entrained air
f = fuel or combustion zone
l = width of plume
m = maximum or center-line value
o = ambient conditions
T = temperature
v = velocity

Superscripts

$\dot{X}$ = signifies rate of change
X' = single prime (per unit length)
X'' = double prime (per unit area)
X''' = triple prime (per unit volume)

ACKNOWLEDGMENT

The authors wish to thank NIST/BFRL for its support.

REFERENCES

1. Quintiere, J.G. and Grove, B.S., "Correlations for Fire Plumes", NIST-GCR-98–744, February 1998.
2. Morton, B.R., Taylor, G.I. and Turner, J.S., "Turbulent Gravitational Convection from Maintained and Instantaneous Sources", in: Proc. of the Royal Soc. of London, Vol. 234 A, 1956, pp. 1–23.
3. Steward, F.R., "Linear Flame Heights for Various Fuels", Combustion and Flame, Vol. 8, 1964, pp. 171–178.
4. Yokoi, S., "Study on the Prevention of Fire Spread Caused by Hot Upward Current", Building Research Report 34, Japanese Ministry of Construction, 1960.
5. Zukoski, E.E., "Properties of Fire Plumes", in: Combustion Fundamentals of Fire, Cox, G. (ed.), Academic Press, London, 1995.
6. Lee, S.L. and Emmons, H.W., "A Study of Natural Convection Above a Line Fire", J. of Fluid Mech., Vol. 11, 1961, pp. 353–368.
7. Taminini F., "Reaction Rates, Air Entrainment and Radiation in Turbulent Fire Plumes", Combustion and Flame, Vol. 30, 1977, pp. 85–101.
8. Heskestad, G., "A Reduced-Scale Mass Fire Experiment", Combustion and Flame, Vol. 83, 1991, pp. 293–301.
9. Zukoski, E.E., "Fluid Dynamic Aspects of Room Fires", First Symposium (International) on Fire Safety Science, 1985, pp. 1–11.
10. Thomas P.H., "The Size of Flames from Natural Fires", Ninth Symposium (International) on Combustion, Academic Press, New York, 1963, pp. 844–859.
11. Hasemi, Y. and Nishita, M. "Fuel Shape Effect on the Deterministic Properties of Turbulent Diffusion Flames", Second Symposium (International) on Fire Safety Science, Hemisphere, New York, 1988, pp. 275–284.
12. Sugawa, O., Yasushi, O. and Satoh, H., "Flame Height from Rectangular Fire Sources Considering Mixing Factor", Third Symposium International on Fire Safety Science, 1991, pp. 435–444.
13. Yuan, L. and Cox, G., "An Experimental Study of Some Line Fires", Fire Safety Journal, Vol. 27, 1996, pp. 123–139.
14. Gore, J.P. and Zhou, X.C., "A Study of Entrainment and Flow Patterns in Pool Fires using Particle Imaging Velocimetry", NIST-GCR-97–706, March 1996.

15. Delichatsios, M.A., "Air Entrainment into Buoyant Jet Flames and Pool Fires", Combustion and Flame, Vol. 70, pp. 33–46.
16. Heskestad, G., "Fire Plumes", in: SFPE Handbook of Fire Protection Engineering (2nd Edn.), National Fire Protection Assoc., Quincy, MA, 1995.
17. Beyler, C.L., "Development and Burning of a Layer of Products of Incomplete Combustion Generated by A Buoyant Diffusion Flame", Thesis, Cambridge, 1983.